Development of Strongly Focused High-Current-Density Ion Beam System and Its Application for the Alpha Particle Measurement in ITER

H. Sakakita 1), S. Kiyama 1), Y. Hirano 1), M. Sasao 2), K. Shinto 2), H. Koguchi 1), Y. Yagi 1), T. Shimada 1), K. Yambe 1), L. Frassinetti 1), A. Okamoto 2), G. Fiksel 3), B. Hudson 3)

1) National Institute of Advanced Industrial Science and Technology (AIST), Tsukuba Central 2, 1-1-1 Umezono, Tsukuba 305-8568, Japan
2) Tohoku University, 6-6-01-2 Aoba, Aramaki, Sendai 980-8579, Japan
3) University of Wisconsin – Madison, Madison, WI 53706, USA

e-mail contact of main author: h.sakakita@aist.go.jp

Abstract. A strongly focused high-current-density ion beam system was successfully developed using large concave electrodes. The beam with a diameter of 345 mm at the electrode is focused into a diameter of ~36 mm at the focal point with a small divergence angle of about ±0.8 deg. In the cases of H^+, He^+ and HeH^+ beams of ~25 keV, it is estimated that the extracted ion current density achieves values as high as ~190, ~86 and ~13 mA/cm^2, respectively. The optimized configuration of the arc chamber gives high performance to the ion source, and an arc efficiency (= beam current /arc power) of more than 1 A /1.5 kW is attained for He^+ beam extraction. To produce a diagnostic helium neutral beam for alpha particle measurement in a nuclear fusion plant based on deuterium-tritium reaction, helium ion (He^+) or helium-hydrogen ion (HeH^+) beams of ~20 keV have been considered as a primary beam. For the He^+ beam, it is important to produce a focused high-current-density ion beam to pass through small apertures of alkali gas cell with a sufficient signal level. For the HeH^+ beam, conditions producing HeH^+ have not been investigated in detail as yet. To extract these beams, a focused high-current-density neutral beam system is used. For HeH^+ beam extraction in the case of ~300 V acceleration, it is found that the production rate of the HeH^+ component increases with the increase in helium gas pressure to total gas pressure ratio when its value is > ~75 %. It is demonstrated for the first time that the current density level of the HeH^+ beam is sufficient for this purpose. To study the effect of irradiation in the case of edge localized mode and/or the disruption, an extreme high-power-density He^+ beam of 248 MW/m^2 and 9.5x10^{21} m^{-2} is irradiated to the plasma facing materials at 1530 mm from the electrode. In particular, in the case of bulk powder metallurgy tungsten, many small holes (ϕ~200 nm) are produced on the tungsten surface, which is observed by a scanning electron microscope. This damage might influence thermal properties, mechanical properties and tritium retention. Therefore, we can recognize that the focused high-current-density ion beam is very useful not only for NBI, but also for diagnostics and material science.

1. Introduction

For the purpose of hydrogen neutral beam injection (NBI) through a narrow port in the vacuum vessel of fusion plasma devices [1,2], we successfully developed a high-current and high-current-density ion beam system with strong focusing characteristics. A considerable amount of ion beams of various elements (hydrogen, deuterium, helium and nitrogen) can also be extracted in this system, which has multi aperture concave-type electrodes and a bucket-type ion source. The beam is strongly focused into a diameter of ~36 mm at the focal point, with a divergence angle of about ±0.8 deg. A power density as high as ~1 GW/m^2 is attained at the focal point of the neutral beam. This type of beam source not only has the capability of producing a strongly focused beam of high current and high current density, but also has the characteristics of high reliability and an excellent beam control property. In Section 2, the detailed characteristics of the high-power-density NBI system are described.

It is very important to measure the behavior of alpha particles, which contribute to the continuous plasma burning in nuclear fusion plants based on deuterium-tritium reaction like ITER. To measure the spatial profiles and velocity distributions of alpha particles, the injection of a permeable helium neutral (He^0) beam of 1-2 MeV into the burning plasma has been considered [3]. The He^0 beam exchanges charges with helium ions (alpha particles), and the energy of the produced high-energy helium neutral particles is measured using an energy analyzer. To produce a diagnostic He^0 beam, the following two methods are being considered. (1) A helium ion (He^+) beam of ~20 keV and ~100 mA/cm^2, used as a primary beam, is converted to a negative helium ion (He^-) beam through the alkali gas cell (conversion rate ~1 %) [3], and accelerated to 1-2 MeV using a radio-frequency quadrupole (RFQ) with focusing and shaping [4], then He^- spontaneously becomes He^0 (~0.2 mA/cm^2) passing through a reasonable length (neutralization efficiency ~20 %). In this system, it is important to produce a focused high-current-density ion beam to pass through small apertures of the alkali gas cell with a sufficient signal level. Therefore, the result on focusing characteristics demonstrated in our beam system has given important information for the construction of a test facility for a He^+ beam system [5].

(2) Another method which can provide a simple way to realize a He^0 beam of 1-2 MeV is to use a helium-hydrogen molecular ion (HeH^+) beam of ~20 keV and ~2 mA/cm^2 as a primary beam. This beam can be accelerated to 1-2 MeV using the RFQ, and neutralized through the gas cell with sufficient probability (neutralization efficiency ~10 %) [3,6]. In this method, the strong focusing characteristics may not be so important, although the divergence of the beam should be as small as possible. This method has considerable advantages, but the conditions for producing a high-current and high-current-density HeH^+ beam have not yet been investigated in a suitable system [7,8]. In Section 3, we will report the results on the optimized conditions for obtaining sufficient HeH^+ beam intensity for alpha particle measurement in ITER using our beam system.

Another application of this focused beam is the irradiation test of materials. In a nuclear fusion plant such as ITER, the thermal flux due to disruption and the edge localized mode (ELM) to the plasma facing materials can cause severe damage to, for example, heat conductivity and mechanical properties. Generally, a heat load test using a high-power-density electron beam has been conducted to plasma facing candidate materials to study the effects of disruption or ELM. However, plasma facing materials are exposed to not only electrons, but also hydrogen isotopes and helium [9]. It has been found that the surface modification induced by hydrogen and helium beam heating is completely different from that by electron beam heating [10]. Recently, it has also been found that helium plasma affects the light reflection properties of a metallic mirror [11]. Therefore, it is very important to irradiate the materials using high-power-density helium and hydrogen beams. By employing our NBI system using helium gas instead of hydrogen gas without gas puffing into the neutralization cell, it is also possible to extract a high-power-density He^+ beam [12]. In Section 4, results on the irradiation of a high-power-density He^+ beam with a disruption heat load level onto plasma facing material candidates (tungsten and ferritic steel) are shown. Finally, a summary is given in Section 5.

2. Characteristics of High-Power-Density Beam System

In our beam system as illustrated in FIG. 1, three sets of multi aperture (with a total of ~3700 holes) concave-type copper electrodes of 345 mm effective diameter, that is, acceleration,

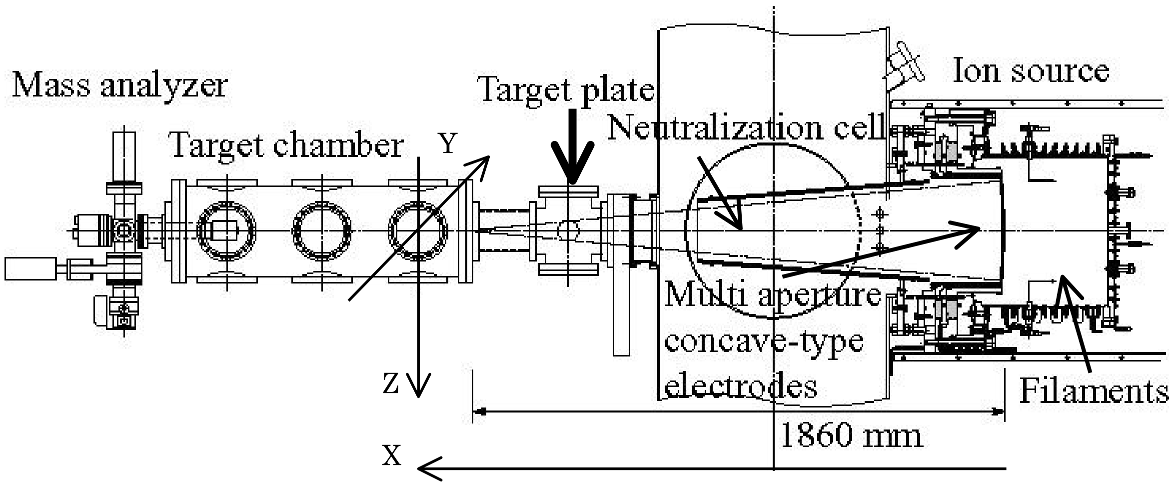

FIG. 1. Schematic drawing of ion beam system.

deceleration and grounded electrodes, are used [2,13]. (Note that, we already developed a high-power-density NBI system using concave-type electrodes whose diameter is 160 mm [1].) The diameter of each extraction aperture on the concave acceleration electrode structure is 4.0 mm on the ion-source side [14]. The transparency of each electrode is ~50 %. The distance between the acceleration and deceleration electrodes is 5.5 mm, and that between the deceleration and grounded electrodes is 2.0 mm. The thickness of all electrodes is 2.0 mm. This aperture configuration may be rather simple and ordinary, but it allows a wide range of operation for the current density, acceleration voltage and gas species. The plasma is produced using a bucket-type ion source whose inside surface is covered by a copper sheet of 2.0 mm thickness to prevent accidental arc erosion. Narrow hairpin tungsten filaments of 2 mm diameter are adopted as cathodes [15], and inserted a few mm inside the plasma region. The cusped magnetic field is larger than 0.15 T at the inside surface of the chamber, and the residual magnetic field in the plasma region is smaller than 0.5 mT. The magnetic field measured using a gauss meter shows a fairly good agreement with the designed value.
A power supply (PS) system with capacitor banks is adopted. The PS specifications are 30 kV and 50 A with voltage ripples of less than 5 % for the acceleration PS, -5 kV and 6 A for the deceleration PS, and 300 V and 1 kA for the arc PS. The filament PS of DC operation (30 s) has the specifications of 20 V and 2700 A (= 180 A x 15 sets of filaments), and a programmed constant-voltage control property with a setting accuracy of 0.1%. The designed beam duration is 35 ms.

Figure 2 shows the time evolutions of the extracted hydrogen ion beam power (P_{beam}). Constant beam extraction with the designed specifications (which correspond to 25 keV, 50 A and 35 ms) is obtained (red line). Here, to keep acceleration voltage (V_{acc}) constant, six resistances of 16.7 Ω each connected in series in the circuit are successively bypassed utilizing IGBT switches; hence, the six-step recovery of V_{acc} is possible. At the maximum beam current (~90 A), the current density becomes as high as 190 mA/cm^2 and a beam power of ~2.1 MW is achieved (blue line). The reduction of beam power after t ~20 ms is due to capacitor limitations. The beam profiles are measured using a thermocouple probe with a ϕ10 mm aperture and a melted pattern of the target plate, which are installed in the target chamber. The movable probes can be swept in X, Y (horizontal) and Z (vertical) directions, as indicated in FIG. 1. The minimum beam diameter is estimated to be ~36 mm from the spot sizes of the beam trace at X = 1383 mm from the electrode (X = 0 mm), as shown in FIG. 3. The beam trajectory is estimated by fitting these beam profile data, as shown in FIG. 4; this gives a beam divergence angle of about ±0.8 deg. The beam power estimated from the beam profile data is in the range of 80 % of that estimated at the electrode. As a result, a power density as high as ~1 GW/m^2 is attained at the focal point of the neutral beam in the case of an extracted current of ~75 A.

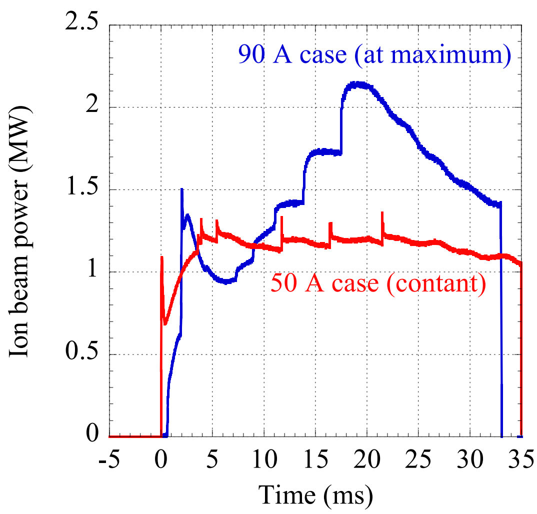

FIG. 2. Time evolutions of hydrogen ion beam power in the case of 50 A (red line) and 90 A (blue line).

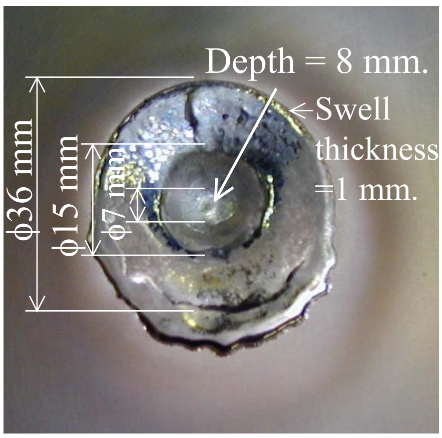

FIG. 3. Beam trace of melted copper target plate.

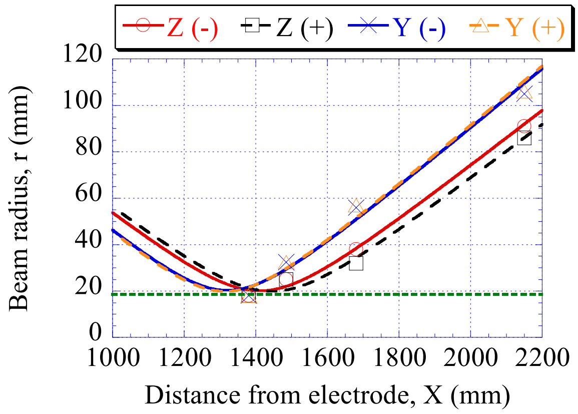

FIG. 4. Beam trajectory estimated by fitting beam profile data obtained by X-, Y- and Z-axis scanning.

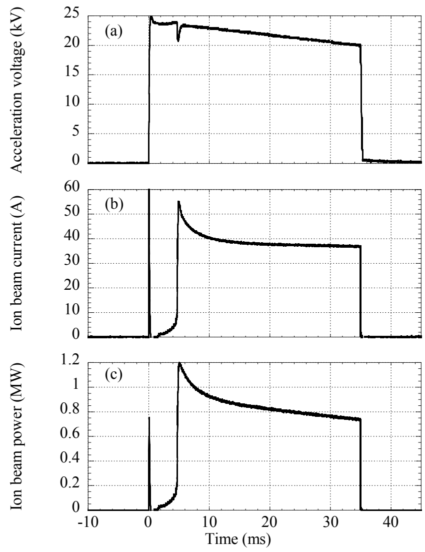

FIG. 5. Time evolutions of (a) acceleration voltage, (b) extracted He+ beam current and (c) ion beam power.

To attain a high-performance ion source, it is important to optimize the configuration of the arc chamber. An arc efficiency (= beam current /arc power) of more than 1 A/1.5 kW is attained for He^+ beam extraction. Figure 5 shows the time evolution of each parameter in the case of V_{acc} = 25 kV, deceleration voltage (V_{dec}) = -1.2 kV, arc voltage (V_{arc}) = 200 V, and filament voltage ($V_{filament}$) = 13.7 V. A He^+ beam of ~22 kV, ~40 A and ~0.8 MW is obtained; then current density corresponds to ~86 mA/cm^2. The most severe problem for the concave-type electrode in operation is that the acceleration (plasma) electrode is heated by the radiation from the filaments and the ion flow to it, and the temperature rise causes the elongation of the electrode and then the considerable reduction of the focal length. To suppress the problem, the electrode is supported by a flexible copper cylinder so that it may expand freely; also, it is also very helpful to raise the arc efficiency.

3. HeH^+ Beam Characteristics for Alpha Particle Measurement

To produce the HeH^+ component in the ion source, helium and hydrogen gases are mixed in the gas reservoir tank at a fixed rate of $P_{He\text{-}ratio}$ which is the ratio of He gas pressure to the total gas pressure of the mixture gas (hydrogen and helium). To measure beam species, a mass and energy analyzer (Balzers Instruments, PPM422) whose maximum energy range is limited to less than 500 eV is used. Therefore, in the case of mass analysis, a DC power supply system of 300 V and 20 A is used as an acceleration PS. Figure 6 shows the time evolution of each parameter in the case of V_{acc} = 300 V, V_{dec} = -4.5 kV, V_{arc} = 110 V, $V_{filament}$ = 10.5 V and $P_{He\text{-}ratio}$ of 75 %. An ion beam of ~6 A and ~1.75 kW, which includes H^+, H_2^+, H_3^+, He^+ and HeH^+ components, is extracted. Figure 7 shows the energy spectrum of HeH^+ particles measured by the mass and energy analyzer for various arc voltages (100 V-150 V), under the same condition as in FIG. 6, except for the arc voltage. The maximum

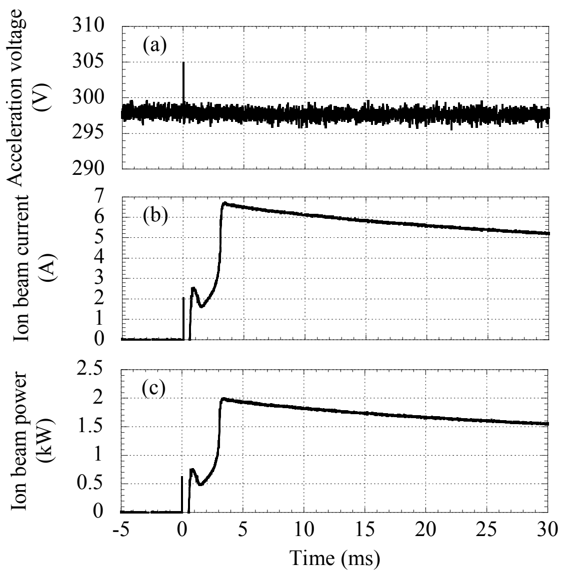

FIG. 6. Time evolutions of (a) acceleration voltage, (b) extracted ion beam current and (c) ion beam power.

number of each particle component may be found in these energy spectra. As the arc voltage increases, the number of HeH^+ particles increases, but saturates at around 130-140 V, which almost corresponds to the electron energy at which the ionization cross section to He^+ becomes maximum. Figure 7 also shows that the peaks of the energy spectrum shift to higher energy with increasing arc voltage. Higher arc voltages may cause a higher space potential in the ion source, which may be favorable for the extraction and convergence of the beam. Figure 8 shows arc power dependency on ion beam current and the numbers of HeH^+ particles in the case of $V_{filament}$ = 10.5 V. As arc power increases, ion beam current increases. (In this arc power region, the current does not saturate.) But, the numbers of particles saturate and somehow decrease. It may be due to the increase of beam divergence which is induced by the increment of extracted current density (namely, self-electric field of ions). Figure 9 shows the numbers of HeH^+, He^+ and H^+ particles as a function of $P_{He\text{-}ratio}$, in the same case as in FIG. 6. It is clear that the production rate of the HeH^+ component increases sharply with increasing $P_{He\text{-}ratio}$ up to ~75 %, and then remains nearly constant up to 90%, whereas those of H^+ and He^+ components are nearly constant in this range of $P_{He\text{-}ratio}$ (50-90 %). This may suggest the mechanism of production in the ion source chamber and of extraction through the electrodes for each component. In the case of $P_{He\text{-}ratio}$ = 90 %, the number of HeH^+ particles corresponds to 15 %, or even more (as the analyzer sensitivity for H^+ may be considerably larger than that for HeH^+), of the total number of H^+, He^+ and HeH^+ particles.

To study the performance of the high-energy beam of ~25 keV, a complex beam with H^+, H_2^+,

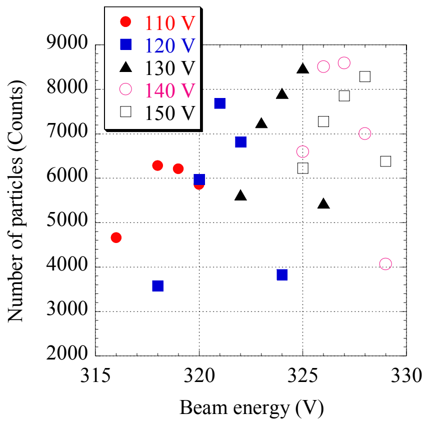

FIG. 7. Energy spectrum of HeH^+ particles measured using a mass and energy analyzer for several arc voltages.

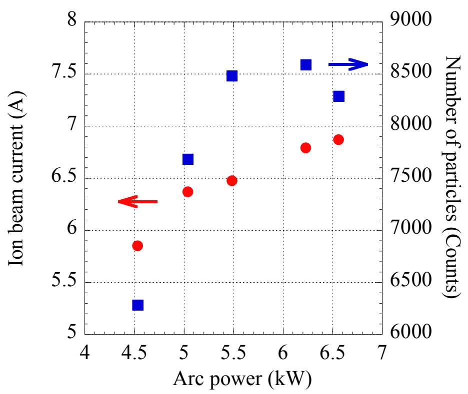

FIG. 8. Arc power dependency on ion beam current (red circles) and the numbers of HeH^+ particles (blue squares).

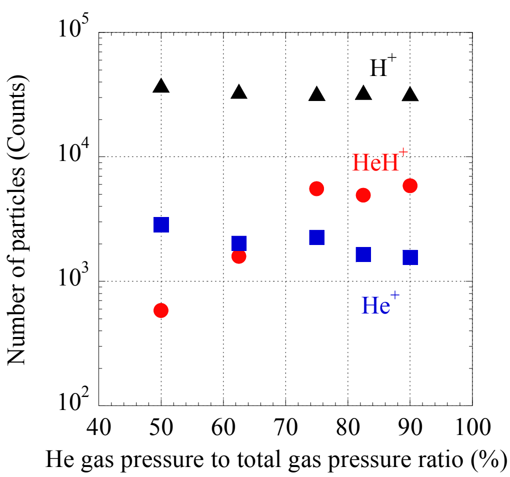

FIG. 9. Numbers of HeH^+ (red), He^+ (blue) and H^+ (black) particles as function of He gas pressure to total gas pressure ratio.

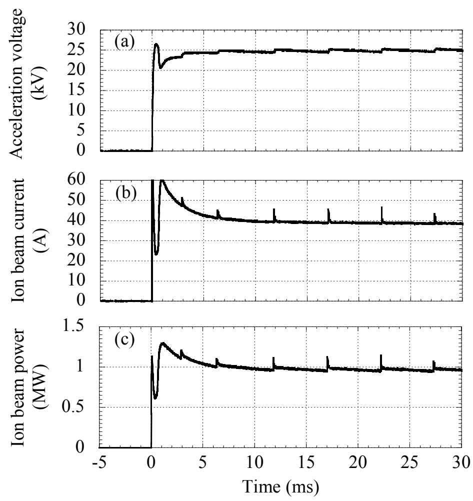

FIG. 10. Time evolutions of (a) acceleration voltage, (b) extracted total ion beam current and (c) total ion beam power.

H_3^+, He^+ and HeH^+ components is extracted. Figure 10 shows the time evolution of each parameter in the case of V_{acc} = 25 kV, V_{dec} = -1.2 kV, V_{arc} = 250 V, $V_{filament}$ = 13.9 V and $P_{He\text{-}ratio}$= 75 %. A total ion beam current of ~40 A with 25 keV is extracted. If 15 % of the total current is assumed to be due to the HeH^+ component, the current density of HeH^+ is estimated as ~13 mA/cm^2, which is much larger than the required value (~2 mA/cm^2) in ITER. However, to verify the estimation, we must directly measure the beam current of the high-energy HeH^+ component, separated from the other components (H^+, H_2^+, H_3^+, He^+) using the magnetic field system.
To examine beam shape, focal point and beam divergence angle, the high-energy beam of ~25 keV is irradiated to the stainless-steel target plates which are installed in the target chamber. The melted patterns on the plates are taken at several positions of distances X= 1530, 1735, 1835 and 1920 mm from the electrodes. From these melted traces, it is estimated that the divergence angle is almost the same as that of the hydrogen beam.

4. Irradiation Experiments of High-Power-Density He^+ Beam to Plasma Facing Material

In the case of a helium discharge, a He^+ beam of ~22 keV and 40 A was obtained and a current density of ~86 mA/cm^2 was achieved, which is described in FIG. 5. At 1530 mm from the electrode, the diameter of the focused He^+ beam is estimated as ~70 mm [7]. Then, the power density (Γ), flux, and total flux are 248 MW/m^2, 6.2x10^{22} m^{-2}s^{-1} and 9.5x10^{21} m^{-2} for 150 ms (= 30 ms x 5 times), respectively. (It is possible to increase the power density to place the materials at the focal point of the beam.) To study the effect of irradiation on the plasma facing materials in the case of the edge localized mode and/or the disruption, this extremely high power density He^+ beam will also be useful.
This high-power-density He^+ beam of level similar to the disruption heat load level in ITER is irradiated to both the bulk powder metallurgy (PM) tungsten (purity ~99.99 %), which is one of the plasma facing candidate materials with low erosion yield and high temperature properties, and ferritic steel. Materials (16.6 x 16.6 mm^2) are placed on the copper plate and fixed by bolts behind the copper plate, as shown in FIGs. 11(a), (b) and (c). The tungsten thickness at the center part is 1 mm with a diameter of 3 mm for tap screw (location (ii)), the thickness of other parts is 3 mm (location (i)). It is easily recognized that the surface of the ferritic steel is completely melted as shown in FIG. 11(c).
Figure 12(a) shows a scanning electron microscope

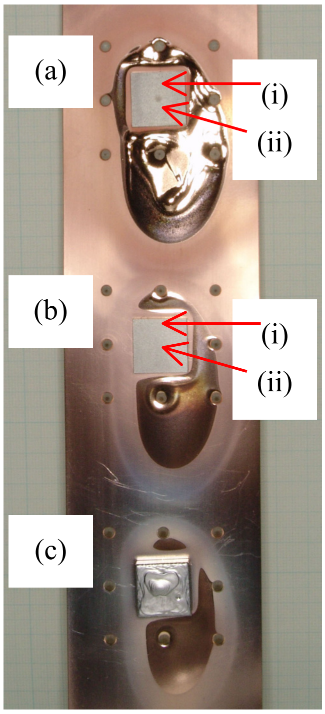

FIG. 11. (a) 5 shots to tungsten, (b) 1 shot to tungsten and (c) 1 shot to ferritic steel.

(a) (b) (c)

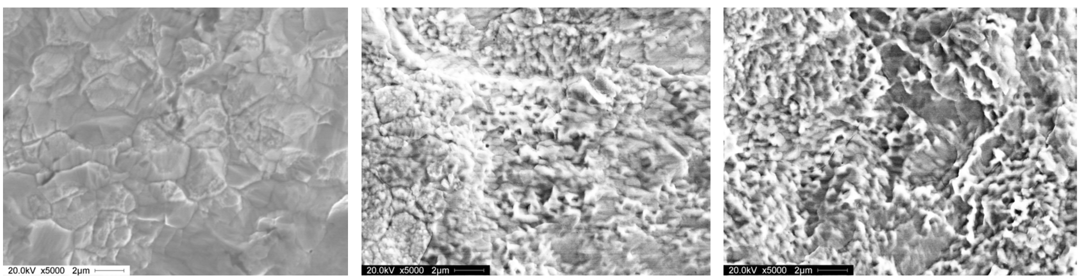

FIG. 12. SEM images (x 5,000) of tungsten surface: (a) before irradiation, (b) location (i) in FIG. 11(b), and (c) location (ii) in FIG. 11(b).

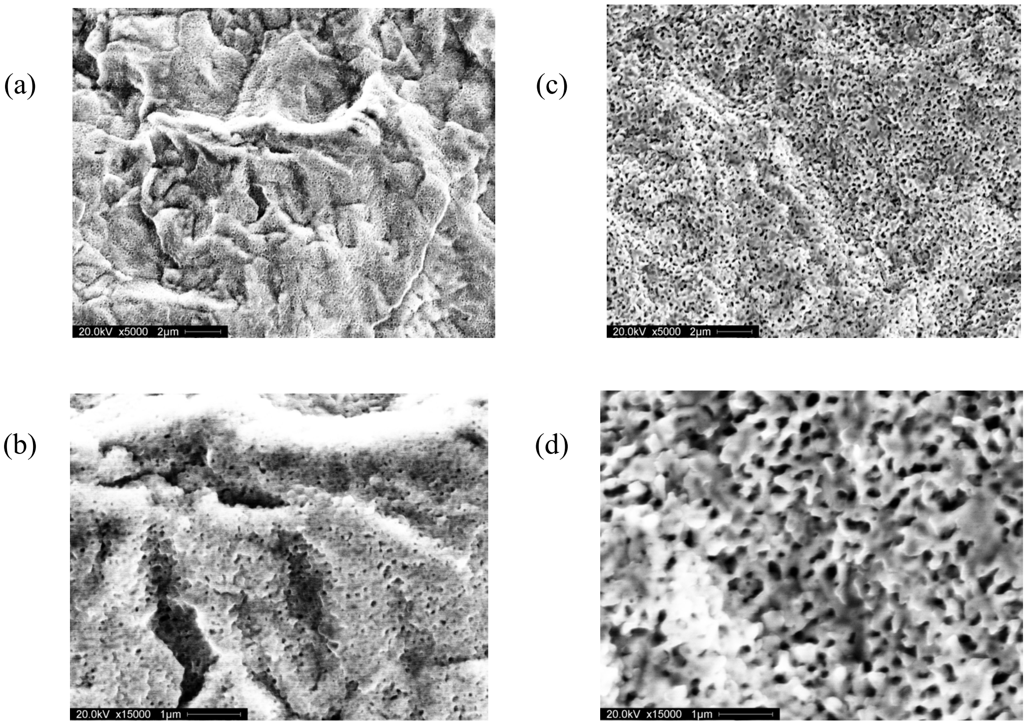

FIG. 13. SEM images of tungsten surface: (a) x 5,000, (b) x 15,000 at location (i) in FIG. 11(a), and (c) x 5,000, (d) x 15,000 at location (ii) in FIG. 11(a).

(SEM) image of the tungsten surface before irradiation. Figures 12(b) and (c) show SEM images of tungsten surface regions which are indicated in (i) and (ii) of FIG. 11(b), respectively, in the case of single-shot He^+ beam irradiation (= 1.9 x 10^{21} m^{-2}). Surface modification and the production of some small holes are shown. In this case, tungsten surface temperature is estimated as ΔT~2689 K using the relation $\Delta T = 2\Gamma\{\tau/(\pi\rho c\kappa)\}^{1/2}$. Here, ρ, c and κ indicate the material density, specific heat and thermal conductivity, respectively.

Figure 13 shows SEM images of tungsten surface regions which are indicated in (i) and (ii) of FIG. 11(a), respectively, in the case of five-shot He^+ beam irradiation (= 9.5 x 10^{21} m^{-2}). The beam is irradiated every 9 minutes. Figures 13(a) and (b) show wide-scale modification and the production of very small holes (< ~100 nm). Figures 13(c) and (d) show that many small holes (ϕ~200 nm) are produced (The center part of the tungsten material in FIG. 11(a)-(ii) looks black). We can understand that the damage becomes more severe, as the thickness of the material becomes thin. This indicates that the temperature of the material is important for enhancing the production rate and size of holes. Thermal conductivity may degrade as the number of beam pulses increases, since the material surface gradually roughens.

5. Summary

A strongly focused high-power-density hydrogen neutral beam system, which has multi aperture concave-type large electrodes and a bucket-type ion source, was successfully developed. It was shown that the neutral hydrogen beam is strongly focused into a diameter of ~36 mm at the focal point with a divergence angle of about ±0.8 deg. As a result, a power density as high as ~1 GW/m^2 was attained at the focal point of the neutral beam.

The characteristics of the HeH^+ beam used as a primary beam, which is converted into a He^0 beam used for the alpha particle diagnostics in ITER, are described. In the case of a low-energy beam of 300 eV, it was found using the mass and energy analyzer that the production rate of the HeH^+ component increases sharply with increasing $P_{He\text{-}ratio}$ up to ~75 %, and then remains nearly constant up to 90%. It was estimated that the number of HeH^+ particles corresponds to more than ~15 % of the total number of H^+, He^+ and HeH^+ particles in the case of $P_{He\text{-}ratio}$ = 90 %. In the case of 25 kV acceleration, if 15 % of the total current (which includes H^+, H_2^+, H_3^+, He^+ and HeH^+ components) is assumed to be due to the HeH^+ component, the current density of HeH^+ is estimated as ~13 mA/cm^2, which is much larger than the required value (~2 mA/cm^2) in ITER. However, to confirm it, we must directly measure the beam current of the high-energy HeH^+ component, separated from the other components (H^+, H_2^+, H_3^+, He^+) using the magnetic field system. This procedure is being performed at present.

A high-power-density He^+ beam of ~248 MW/m^2 was successfully extracted using an NBI system with large-area concave electrodes. This high-power-density He^+ beam was irradiated to PM tungsten and ferritic steel. Even in the case of 1.9 x 10^{21} m^{-2} flux, this high-power-density He^+ beam causes severe damage to the surface of tungsten material. It was also found that hole sizes on the surface depend on the amount of total flux and the thickness of the material. This damage might influence thermal properties, mechanical properties and tritium retention. It was easily recognized that the surface of the ferritic steel is completely melted at one shot. As future plans, the following are considered: irradiation experiments using a hydrogen beam, a hydrogen and helium mixture beam and an electron beam, cross-sectional image observation by transmission electron microscope, and successive irradiation experiments using a short-pulse beam (a few ms) with a high power density (ELM simulator), among others.

Therefore, we can recognize that focused high-current-density ion beams are very useful not only for NBI, but also for diagnostics and material science.

Acknowledgement

A part of this study was financially supported by the Budget for Nuclear Research of the Ministry of Education, Culture, Sports, Science and Technology of Japan, based on the screening and counseling of the Atomic Energy Commission, and a part of this study was financially supported by the Grant-in-Aid for Scientific Research from the Japan Society for the Promotion of Science. We thank Professor S. Goto of Osaka University for helpful advice regarding the beam electrode.

References

[1] SAKAKITA, H., et al., Proc. 30th Eur. Phys. Conf. on Control. Fusion and Plasma Phys., **27A**, St Petersburg, P2-173 (2003).
[2] SAKAKITA, H., et al., Proc. 32nd Eur. Phys. Conf. on Control. Fusion and Plasma Phys., Tarragona, P4-109 (2005).
[3] SASAO, M., et al., Proc. Int. Workshop on Diagnostics for ITER, Varenna (2005) 51.
[4] MAEBARA, S., et al., Proc. Particle Accelerator Conf., Knoxville (2005) 904.
[5] SHINTO, K., et al., Proc. 9th IAEA Technical Meeting on Energetic Particles in the Magnetic Confinement Systems, Takayama, P21 (2005).
[6] WARREN, J., et al., Phys. Rev. A **4** (1971) 1960.
[7] SAKAKITA, H., et al., Proc. 9th IAEA Technical Meeting on Energetic Particles in the Magnetic Confinement Systems, Takayama, P20 (2005).
[8] SAKAKITA, H., et al., Proc. 33rd Eur. Phys. Conf. on Control. Fusion and Plasma Phys., Roma, P1-123 (2006).
[9] NISHIJIMA, D., et al., Jpn. J. Appl. Phys. **44** (2005) 380.
[10] TOKUNAGA, K., et al., J. Nucl. Materials 329-333 (2004) 757.
[11] EBIHARA, A., et al., Proc. Fusion Energy Conf., Toyama, 14G31 (2006) 141 [in Japanese].
[12] SAKAKITA, H., et al., Proc. 33rd Eur. Phys. Conf. on Control. Fusion and Plasma Phys., Roma, P1-115 (2006).
[13] NISHIKAWA, M., et al., Fusion Eng. Des. **16** (1991) 351.
[14] COUPLAND, J.R., et al., Rev. Sci. Instrum. **44** (1973) 1258.
[15] KURIYAMA, M., et al., JAERI Reports, JAERI-M87 (1987) 169 [in Japanese].